



Article

Joint Component Estimation for Electricity Price Forecasting Using Functional Models

Francesco Lisi ^{1,*}  and Ismail Shah ^{1,2,*} ¹ Department of Statistical Sciences, University of Padua, 35121 Padua, Italy² Department of Statistics, Quaid-i-Azam University, Islamabad 45320, Pakistan

* Correspondence: francesco.lisi@unipd.it (F.L.); ismail.shah@unipd.it (I.S.)

Abstract: This work considers the issue of modeling and forecasting electricity prices within the functional time series approach. As this is often performed by estimating and predicting the different components of the price dynamics, we study whether jointly modeling the components, able to account for their inter-relations, could improve prediction with respect to a separate instance of modeling. To investigate this issue, we consider and compare the predictive performance of four different predictors. The first two, namely Smoothing Splines-Seasonal Autoregressive (SS-SAR) and Smoothing Splines-Functional Autoregressive (SS-FAR) are based on separate modeling while the third one is derived from a single-step procedure that jointly estimates all the components by suitably including exogenous variables. It is called Functional Autoregressive with eXogenous variables (FARX) model. The fourth one is a combination of the SS-FAR and FARX predictors. The predictive performances of the models are tested using electricity price data from the northern zone of the Italian electricity market (IPEX), both in terms of forecasting error indicators (MAE, MAPE and RMSE) and by means of the Diebold and Mariano test. The results point out that jointly estimating the components leads to significantly more accurate predictions than using a separate instance of modeling. In particular, the MAE, MAPE, and RMSE values for the best predictor, based on the FARX(3, 0, 4) model, are 4.25, 9.28, and 5.38, respectively. The percentage error reduction is about 20% with respect to SS-SAR(3, 1) and about 10% with respect to SS-FAR(5). Finally, this study suggests that the forecasting errors are generally higher on Sunday and Monday, from hours 3 to 6 in the morning and 14 to 15 in the afternoon, and in June and December. On the other hand, prices are relatively lower on Wednesday, Thursday, and Friday, from hour 20 to 1 a.m., and in January and February.



Citation: Lisi, F.; Shah, I. Joint Component Estimation for Electricity Price Forecasting Using Functional Models. *Energies* **2024**, *17*, 3461. <https://doi.org/10.3390/en17143461>

Academic Editor: Seung-Hoon Yoo

Received: 29 May 2024

Revised: 8 July 2024

Accepted: 11 July 2024

Published: 14 July 2024



Copyright: © 2024 by the authors. Licensee MDPI, Basel, Switzerland. This article is an open access article distributed under the terms and conditions of the Creative Commons Attribution (CC BY) license (<https://creativecommons.org/licenses/by/4.0/>).

Keywords: electricity prices; functional autoregressive model; functional autoregressive with exogenous variables model; functional principal components; vector autoregressive model

1. Introduction

Electricity price forecasting is an important issue for producers and consumers in today's competitive electricity markets. As electricity cannot be efficiently and economically stored in large quantities using current technologies, a slight shift in demand can result in a massive change in electricity prices and, hence, pose a significant risk for traders in the markets. Accurate forecasts empower energy companies to optimize their production schedules, mitigate risks, and make informed trading decisions. Moreover, the end consumers also benefit from improved budgeting and strategic consumption planning. Meanwhile, electricity price forecasting is a challenging task due to its specific features [1].

It is well known that time series of electricity prices are characterized by both long-term and periodic (yearly, weekly, and daily) behaviors, calendar effect, spikes and/or level shifts as well as short-term serial dependence [2,3]. All these components have been considered in several ways in the literature, but we can divide them into methods considering some components as deterministic and others as stochastic, and methods that model all the components as stochastic. In the first case, the usual approach is filtering the

deterministic components by some procedure, for example, using smoothing spline and stochastically modeling the residual component [4]. For example, ref. [5] proposed a semi-parametric component-based model consisting of a non-parametric (smoothing spline) and a parametric (autoregressive moving average (ARMA) model) component. To capture different characteristics of day-ahead electricity prices, ref. [6] proposed a model based on the improved empirical mode decomposition (IEMD), ARMA with exogenous terms (ARMAX), exponential generalized autoregressive conditional heteroscedasticity (EGARCH) and adaptive network-based fuzzy inference system (ANFIS). The non-parametric regression techniques and semi-functional partial linear models are used by [7] for electricity demand and price prediction. In this case, the deterministic components are filtered out first, and then the residual component is modeled with a suitable stochastic process.

In the second case, all components are jointly accounted by a single stochastic model [8–10]. For instance, ref. [11] studied the periodic behavior of the electricity prices using the seasonal Reg-ARFIMA-GARCH model that explains the conditional mean and variance of electricity prices. Ref. [12] studied the performance of AR-GARCH models on the Indian spot electricity price series. Different seasonalities are captured in the model using hourly, weekly, and daily dummy variables. The conditional mean and conditional variance equations for different variants of the model are estimated, and the forecasting performance of the calibrated models is assessed using standard accuracy measures. The study suggested that AR-GARCH and AR-EGARCH outperform the competitors. Ref. [13] compared the forecasting performance of different approaches, including transfer function, ARIMA, wavelet, and artificial NN used for electricity price forecasting. Ref. [14] studied the performance of univariate time series models for forecasting electricity demand using both components jointly.

Apart from the two approaches described above, researchers used different classical and machine learning techniques to model and forecast electricity prices [15–17]. For instance, ref. [18] performed short-term price prediction using regression trees to predict the electricity price. The results of the proposed method are compared with alternative methods like ARIMA, exponential smoothing, and neural networks (NN). The empirical results show that the proposed method performs better than the competitors. Ref. [19] used a variable-segmented support vector machine-based model (VS-SVM) for day-ahead price forecasting in Ontario's electricity market. The author used the heuristic model, simulation model (Monte Carlo simulation approach), multiple linear regression (MLR), NN model, neuro-fuzzy, ARIMA, dynamic regression model (DRM), and transfer function model (TFM) to compare with the proposed hybrid model. The results indicated that the VS-SVM model outperformed all the other models in terms of MAPE and RMSE. Ref. [20] proposed a fuzzy neural network-based method for short-term price forecasting for mainland Spain's electricity market. The author compared the proposed model with other fuzzy regression models and hybrid approaches based on NN and fuzzy logic, ARIMA, wavelet-ARIMA, multi-layer perceptron (MLP) and radial basis function (RBF) neural networks. The results indicated that the proposed method outperformed other methods in terms of forecasting accuracy and robustness against outliers and non-stationary behavior of the price series. The use of these forecasting models is not limited to the electricity market as they are extensively used in other research fields [21–23]. A summary of previous studies concerning electricity market forecasting is given in Table 1.

In the last years, a promising approach to deal with the complex behavior of electricity markets time series is that based on functional data analysis. Functional modeling can handle high-dimensional data and facilitates the transformation of long forecast horizons into a one-step-ahead functional forecast [24,25]. Considering functional data allows one to obtain forecasts for ultra-short periods, which is not possible with traditional techniques. In addition, it is particularly useful to describe daily periodic profiles of some market variables. In the electricity prices time series literature, when the functional approach has been involved, the separate estimation has always been used. While a separate estimation permits to highlight the role of each component, a joint estimation could account for those inter-relations among components that a separate modeling process usually ignores,

possibly improving prediction. In this work, we try to fill the gap by suggesting a functional model that allows for the joint estimation of the components. To investigate the issue, we consider and compare the predictive performance of different predictors referring to both the separate and the joint component estimation. In more detail, we consider two models based on the separate component estimation which use smoothing splines (SS) in the first step and SARIMA (SS-SAR) models or standard functional autoregressive (SS-FAR) models in the second step. For the joint estimation, we consider an extension of the standard FAR model which includes exogenous variables describing the deterministic components (FARX). A suitable estimation procedure based on principal components is proposed. For a deeper insight, we also consider a predictor based on a combination of the two approaches. We test the predictive performances of the models on the hourly electricity prices of the northern zone of the Italian electricity market (IPEX) and show that, using functional models, the joint components estimation leads to significantly better prediction than the separate estimation.

Table 1. Summary of literature review.

No.	Authors	Market	Forecasting	Methods	Accuracy Measures
1	Marcjasz et al. (2023) [26]	Germany	Day-ahead	DNN	MAE, RMSE, CRPS
2	Alberto et al. (2011) [27]	Spain	Day-ahead	double seasonal ARIMA, ES model	SSR, MAPE
3	Girish (2016) [12]	India	Hour-ahead	AR-GARCH, ARIMA-EGARCH	RMSE, MAE, MAPE
4	Zhang et al. (2019) [5]	Spain, Australia	Day-ahead	IEMD, ARMAX, EGARCH, ANFIS	MAE, RMSE, MAPE
5	Aggarwal et al. (2009) [19]	Canada	Hour-Ahead	VS-SVM, MLR, NN, DRM	RMSE, MAPE
6	Amjady (2006) [20]	Spain	Day-ahead	ARIMA, Wavelet-ARIMA, MLP, RBF	TE, DME
7	Shah et al. (2020) [28]	Italy	Day-ahead	AR, NPAR, FAR, NPFAR	MAE, MAPE, R ²
8	Vilar et al. (2012) [7]	Spain	Day-ahead	ARIMA, FNP, SFPL	DEs, SE
9	Conejo et al. (2005) [29]	Spain	Day-ahead	wavelet transform, ARIMA	DEs, HE
10	Dudek (2015) [18]	Poland	Day-ahead	RF, ARIMA, ES, NN	RMSE

Distributional Neural Networks (DNN), Exponential Smoothing (ES), Continuous Ranked Probability Score (CRPS), Sum of Squared Residuals (SSR), Training Error (TE), Daily Mean Error (DME), Functional Non-parametric (FNP), Semi-Functional Partial Linear (SFPL), Daily Errors (DEs), Seasonal Error (SE), Hourly Error (HE), Random Forest (RF).

The rest of the paper is structured as follows. The general framework within which we move is described in Section 2. Section 3 provides a basic introduction to functional data and the details of the functional models we use. The description of the data, as well as of our forecasting exercise, are contained in Section 4. Section 5 concludes the paper.

2. General Framework

The general framework within which we move in this work is the following.

Let us denote by $P_{t,j}$ the time series of the price for day t and load period (hour) h , $t = 1, \dots, n$ and $h = 1, \dots, 24$. We assume that its logarithm, $\log(P_{t,j})$, can be decomposed in several additive components:

$$\log(P_{t,j}) = T_{t,j} + Y_{t,j} + W_{t,j} + C_{t,j} + p_{t,j} \quad (1)$$

where $T_{t,j}$ represents the long-run (trend component), $Y_{t,j}$ is the annual periodic component, $W_{t,j}$ is the weekly cycles, $C_{t,j}$ is the calendar component describing the effect of bank holidays and other possible calendar effects. Finally, $p_{t,j}$ describes the short-run dynamics of the price series. Note that since expression (1) refers to a given time slot j , the daily component, due to the periodicity over the hours of the day, is not present. This is why, in the rest of the work, when not necessary, we will omit the hour subscript j .

Usually, the trend is represented through the sequence $1, 2, \dots, n$, the yearly component by the sequence $(1, \dots, 365, 1, \dots, 365, \dots)$ or by trigonometric functions, the weekly period by the sequence $(1, \dots, 7, 1, \dots, 7, \dots)$, while bank holidays are described by dummy variables.

In the literature, these components have been treated in several ways: using different models or approaches, assuming that the first four components are deterministic while the residual component is stochastic [30] or treating all components as stochastic [31],

estimating them separately or jointly. In this work, we compare the predictive performance of functional models when the components are separately or jointly modeled. To the best of our knowledge, the joint estimation of the components using functional methods is new within energy markets.

In the separate approach, the deterministic and the stochastic components are usually estimated using a two-step procedure. First the deterministic components are estimated, then the stochastic component is obtained as the residual difference

$$p_{t,j} = \log(P_{t,j}) - \hat{T}_{t,j} + \hat{Y}_{t,j} + \hat{W}_{t,j} + \hat{C}_{t,j}. \quad (2)$$

The series p_t are then modeled following some stochastic approach.

In this work, for each given time period j , we estimate the deterministic components using the non-parametric additive model:

$$\log(P_t) = f_1(T_t) + f_2(Y_t) + f_3(W_t) + \delta(C_t) + \varepsilon_t, \quad (3)$$

where δ is a constant parameter defining the bank holidays effect and f_i are functions describing the relations between $\log(P_t)$, which are jointly estimated through smoothing splines.

After the residual component $p_{t,j}$ has been estimated using expression (2), we put together the series $p_{t,j}$ to convert them in functional time series. To this end, we use B-spline basis functions, so that we can write

$$p_t(\tau) = \sum_{k=1}^K C_{tk} \phi_{tk}(\tau) \quad (4)$$

where C_{tk} are constant parameters, $\phi_{tk}(\tau)$ represent the B-spline basis functions, and K is the number of basis functions used.

Once the functional time series $p_t(\tau)$ is available, we model it by means of functional autoregressive models (FAR).

The final prediction is obtained by summing the individual forecast:

$$\hat{P}_{t+1,j} = \exp\left(\hat{f}_1(T_{t+1}) + \hat{f}_2(Y_{t+1}) + \hat{f}_3(W_{t+1}) + \delta(C_{t+1}) + \hat{p}_{t+1,j}\right). \quad (5)$$

When the joint estimation approach is considered, both deterministic and stochastic components are estimated using a single-step procedure. This helps to account for possible relationships between deterministic and stochastic components. While joint estimation of the components is not a novelty, it is new in the energy field using functional models.

For the joint estimation, we consider a functional autoregressive model with suitable exogenous variables (FARX), allowing us to include the effects of scalar or functional exogenous drivers. The estimation of such a model is challenging since the computational burden increases more than linearly with the lag orders of endogenous and exogenous variables. In addition, in many cases, the estimation is unfeasible due to the unboundedness of the inverse of covariance operators. Thus, a feasible and adaptable strategy is required. In this work, we use the principle component analysis (PCA) to reduce the number of variables while retaining most information included in the endogenous and exogenous variables. In this case, first $\log(P_{t,j})$ is converted into a functional time series using the methodology explained in Section 2 and, then, a suitable FARX model is estimated using the PCA approach. The estimated model also allows for the series prediction.

3. Functional Data Analysis

3.1. Preliminaries

This section provides a basic introduction to functional data analysis which is essential to understand the contents of this work. In the following, we will use the *mathcal* font

to denote functional objects, bold fonts for vectors and matrices, and normal fonts for scalar quantities.

Let $\mathcal{Z}_t(\tau)$ be a time series of functional observations, where $\tau \in [a, b]$ and $t \in \mathbb{N}$. Usually the interval $[a, b]$ is normalized to $[0, 1]$. For each t , the observation $\mathcal{Z}_t(\tau)$ belongs to the Hilbert space $\mathbb{H} \in L^2([0, 1], \|\cdot\|)$ of square integrable functions which is equipped with a norm $\|\cdot\|$ induced by the inner product $\langle x, z \rangle = \int x(t)z(t)dt$.

For a generic time series $\mathcal{Z}_t(\tau)$, defined on a probability space $(\Omega, \mathcal{A}, \mathcal{P})$, with mean function $E[\mathcal{Z}_t(\tau)] = \mu(\tau)$, the covariance function $C(\mathcal{X})$, with $x \in L^2[0, 1]$, is defined as

$$C(\mathcal{X}) = E[\langle \mathcal{Z}_t(\tau) - \mu, \mathcal{X} \rangle \mathcal{Z}_t(\tau) - \mu] \quad (6)$$

The covariance function (6) can also be expressed using the following spectral decomposition:

$$C(\mathcal{X}) = \sum_{k=1}^{\infty} \lambda_k \langle \phi_k, x \rangle \phi_k \quad (7)$$

where $\langle \cdot, \cdot \rangle$ is the inner product, $\{\lambda_k\}_{k \geq 1}$ is the strictly positive decreasing sequence of eigenvalues of (6) and $\{\phi_k\}_{k \geq 1}$ denotes the corresponding sequence of eigenfunctions which form an orthonormal basis system for \mathbb{H} .

The functional time series $\mathcal{Z}_t(\tau)$ can also be represented using the principal component approach, based on the Karhunen-Loève representation [32]. If $\mathcal{Z}_t^*(\tau) = \mathcal{Z}_t(\tau) - \mu(\tau)$, we can write:

$$\mathcal{Z}_t^*(\tau) = \sum_{k=1}^{\infty} y_{k,t} \phi_k(\tau), \quad (8)$$

where $y_{k,t} = \int \mathcal{Z}_t^*(\tau) \phi_k(\tau) d\tau$ denotes the k^{th} functional principal component score while $\phi_k(\tau)$ are the function principal components (FPC). The functional principal component constitutes an uncorrelated set of random variables with zero mean and variance λ_k . The λ_k s are such that $\lambda_1 \geq \lambda_2 \geq \lambda_3 \geq \dots$

The main advantage of expansion (8) is it allows dimension reduction as the first d terms often provide a good enough approximation to the infinite sum and, thus, the information contained in \mathcal{Z}_t^* can be adequately summarized considering only the first d principal components. The approximated process is given by

$$\mathcal{Z}_t^*(\tau) \approx \sum_{k=1}^d y_{k,t} \phi_k(\tau), \quad (9)$$

More details on functional principal components and their practical applications are given in [33,34].

In practice, all the previously defined quantities have to be estimated starting from an observed time series, $\mathcal{Z}_1^*(\tau), \dots, \mathcal{Z}_n^*(\tau)$, representing a finite realization of the underlying random process. To this end, the following estimators can be used:

$$\hat{\mu}(\tau) = \frac{1}{n} \sum_{i=1}^n \mathcal{Z}_i(\tau), \quad (10)$$

$$\hat{C}_n(x) = \frac{1}{n} \sum_{i=1}^n \langle \mathcal{Z}_i(\tau), x \rangle (\mathcal{Z}_i(\tau)). \quad (11)$$

The authors of [35] showed that the estimators (10) and (11) are consistent estimators for weekly dependent processes. Then, using the KL expansion, the realizations of the random process $\hat{\mathcal{Z}}_t^*(\tau)$ can be written as

$$\hat{\mathcal{Z}}_t^*(\tau) = \sum_{k=1}^d \hat{y}_{k,t} \hat{\phi}_k(\tau) + \hat{\varepsilon}(\tau), \quad i = 1, 2, \dots, N \quad (12)$$

where $\hat{y}_{k,t}$ is the k^{th} estimated functional principle component score for the t^{th} observation, $\hat{\phi}_k(\tau)$ is the k^{th} functional principle components and $\hat{\epsilon}(\tau)$ is an estimated white noise. This formulation allows us to describe the FAR and FARX models, which will be used to forecast $Z_t^*(\tau)$.

3.2. Functional Autoregressive Models

One of the simplest ways to model a functional time series $Z_t(\tau)$ is to use a functional autoregressive model of order p , $FAR(p)$ [36]. A $FAR(p)$ model, which is the generalization of an $AR(p)$ model to the case of functional objects, is defined as

$$Z_t(\tau) = \sum_{j=1}^p \Psi_j Z_{t-j}(\tau) + \mathcal{N}_t(\tau) \quad (13)$$

where $\Psi_j (j = 1, \dots, p)$ are the functional parameters of the model, $Z_{t-j}(\tau)$ are lagged functional variables and $\mathcal{N}_t(\tau)$ is a strong \mathbb{H} -white noise with zero mean and finite second moment ($E\|\mathcal{N}_t(\tau)\|^2 < \infty$). The $FAR(p)$ model can be further generalized by including, besides Z_{t-j} lagged variables, other exogenous (possibly lagged) regressors. These exogenous variables may be scalars (X_t), vector-valued (\mathbf{X}_t) or functional (\mathcal{X}_t). The $FARX(p, m, r)$ model can be defined as

$$Z_t(\tau) = \sum_{j=1}^p \Psi_j Z_{t-j}(\tau) + \sum_{i=1}^m \mathbf{B}_i \mathcal{X}_i(\tau) + \sum_{k=1}^r \gamma_k X_k + \mathcal{N}_t(\tau) \quad (14)$$

where $\mathcal{X}_i(\tau)$ denotes the functional exogenous variables, X_j are the scalar exogenous variables and $\mathcal{N}_t(\tau)$ is a strong \mathbb{H} -white noise as in (14). Often, the exogenous variables are previously demeaned. Ψ_j , ($j = 1, \dots, p$), \mathbf{B}_i , ($i = 1, \dots, m$) and γ_k , ($j = 1, \dots, r$) are functional (the first two) and scalar (the third one) model parameters.

3.3. Building $FAR(p)$ and $FARX(p, m, r)$ Models

Building FAR and FARX models requires one to identify the orders p , m and r as well as to estimate the model parameters. A partial theoretical estimation procedure for $FAR(p)$ is given in [36]. This is based on the Shibata-Mourid [37] statistics; however, practical estimation issues are completely ignored by the author. The procedure works in the case of $FAR(1)$; however, it is not clear how to apply it to real data for generic $FAR(p)$ models. In the case of $FAR(1)$, the PCs' use is useful since the covariance operator behaves erratically due to the unboundedness of its inverse, and thus, the data are projected onto a suitable finite-dimensional subspace, generally spanned by the first few largest eigenvectors.

In this work, we estimate the $FAR(p)$ and $FARX(p, m, r)$ using the principle components approach. This ensures a fair model estimation as well as computational efficiency since most of the variation in the endogenous and exogenous variables is summarized by the first PCs. Clearly, in this case, the identification step requires the selection of the lag orders (p, m, r) and the number of FPCs (d) used in the approximation. To this end, to select p and d , the following algorithm is used

1. (a) For a demeaned functional dataset $Z_t(\tau)$, fix a dimension d and, using (8), compute the vector $\hat{\mathbf{Y}}_t = (\hat{y}_{1,t}, \dots, \hat{y}_{d,t})'$, containing the first d FPC scores.
- (b) For each functional exogenous variables fix the value of m and use the data $\mathcal{X}_i(\tau)$ to compute the vector $\hat{\mathbf{A}}_i = (\hat{A}_{k,1}, \dots, \hat{A}_{k,m})'$, containing the first m FPC scores of the exogenous variable lag matrix.
- (c) combine all the exogenous variables vectors into a single vector, $\hat{\mathbf{B}} = (\hat{\mathbf{A}}_i, X_k)'$,
2. Using $\hat{\mathbf{Y}}_1, \dots, \hat{\mathbf{Y}}_t$ and $\hat{\mathbf{B}}$, consider an appropriate multivariate model, for example vector autoregressive model, $\mathbf{Y}_t = \sum_{j=1}^p \Psi_j \mathbf{Y}_{t-j} + \epsilon_t$, to obtain a one-step ahead forecast for \mathbf{Y}_{t+1} as

$$\hat{\mathbf{Y}}_{t+1} = (\hat{y}_{t+1,1}, \dots, \hat{y}_{t+1,d})'$$

- Choose the order p and d using Section 3.4 and obtain \mathbf{Y}_{t+1} for the optimal p and d .
- Use the KL expansion to compute the one-step-ahead forecast

$$\hat{\mathbf{Z}}_{t+1} = \hat{\mu}(t) + \hat{y}_{t+1,1}\hat{\phi}_1 + \dots + \hat{y}_{t+1,d}\hat{\phi}_d.$$

3.4. Selection of Orders p, m, r and Number of PCs d

The performance of functional models FAR(p) and FARX(p, m, r) crucially depends on the appropriate selection of the order p, m, r and of the suitable number of PCs d . In this section, we show that they can be jointly estimated using the functional final prediction error (FFPE) criterion.

We start by considering the mean squared error (MSE). Since the eigenfunctions ϕ_i are orthogonal and the PCs $y_{k,t}$ are uncorrelated, it can be written as

$$\begin{aligned} \mathbb{E}\left\{\left\|\mathbf{Z}_{t+1}(\tau) - \hat{\mathbf{Z}}_{t+1}(\tau)\right\|^2\right\} &= \mathbb{E}\left\{\left\|\sum_{k=1}^{\infty} y_{t+1,k}\phi_k - \sum_{k=1}^d \hat{y}_{t+1,k}\phi_k\right\|^2\right\} \\ &= \mathbb{E}\left\{\left\|\mathbf{Z}_{t+1} - \hat{\mathbf{Z}}_{t+1}\right\|^2\right\} + \sum_{k=d+1}^{\infty} \lambda_k. \end{aligned}$$

Here, the usual L^2 Euclidean norm of vectors is represented by $\|\cdot\|^2$. Assuming the stationarity of the process \mathbf{Z}_t , a d -variate VAR(p) has the form

$$\mathbf{Z}_{t+1} = \Psi_1\mathbf{Z}_t + \Psi_2\mathbf{Z}_{t-1} + \dots + \Psi_p\mathbf{Z}_{t-p+1} + \zeta_{t+1}$$

where ζ_t is a white noise process such that [38]

$$\sqrt{t}(\hat{\rho} - \rho) \xrightarrow{D} \mathbf{N}_{p*d^2}(\mathbf{0}, \Sigma_{\zeta} \otimes \Delta_p^{-1}) \tag{15}$$

where $\hat{\rho} = \text{vec} [\hat{\Psi}_1, \dots, \hat{\Psi}_p]'$ is the least squares estimator of $\rho = \text{vec} [\Psi_1, \dots, \Psi_p]'$, and $\Delta_p = \text{Var}[\text{vec}(\mathbf{Z}_1, \dots, \mathbf{Z}_p)]$ and $\Sigma_{\zeta} = E[\zeta_1, \zeta_1']$. Suppose that the $\hat{\rho}$ are estimated from independent training sample $(\mathbf{R}_1, \dots, \mathbf{R}_t) \stackrel{D}{=} (\mathbf{Z}_1, \dots, \mathbf{Z}_t)$. It follows then

$$\begin{aligned} \mathbb{E}\left\{\left\|\mathbf{Z}_{t+1} - \hat{\mathbf{Z}}_{t+1}\right\|^2\right\} &= \mathbb{E}\left\{\left\|\mathbf{Z}_{t+1} - (\hat{\Psi}_1\mathbf{Z}_t + \dots + \hat{\Psi}_p\mathbf{Z}_{t-p+1})\right\|^2\right\} \\ &= \mathbb{E}\left\{\left\|\zeta_{t+1}\right\|^2\right\} + \mathbb{E}\left\{\left\|(\Psi_1 - \hat{\Psi}_1)\mathbf{Z}_t + \dots + (\Psi_p - \hat{\Psi}_p)\mathbf{Z}_{t-p+1}\right\|^2\right\} \\ &= \text{trace}\{\Sigma_{\zeta}\} + \mathbb{E}\left\{\left\|[I_p \otimes (\mathbf{Z}'_t, \dots, \mathbf{Z}'_{t-p+1})](\rho - \hat{\rho})\right\|^2\right\} \end{aligned} \tag{16}$$

The independence of $\hat{\rho}$ and $(\mathbf{Z}_1, \dots, \mathbf{Z}_t)$ yields that

$$\begin{aligned} \mathbb{E}\left\{\left\|[I_p \otimes (\mathbf{Z}'_t, \dots, \mathbf{Z}'_{t-p+1})](\rho - \hat{\rho})\right\|^2\right\} &= \mathbb{E}\left[\text{trace}\left\{(\rho - \hat{\rho})' [I_p \otimes \Gamma_p] (\rho - \hat{\rho})\right\}\right] \\ &= \text{trace}[I_p \otimes \Gamma_p] \mathbb{E}[(\rho - \hat{\rho})(\rho - \hat{\rho})'] \end{aligned}$$

By using (15), the last term can be approximated as

$$\frac{1}{t} \left(\text{trace} [\Sigma_{\zeta} \otimes I_{pd}] + o(1) \right) \sim \frac{pd}{t} \text{trace}(\Sigma_{\zeta}).$$

Replacing $\text{trace}(\Sigma_{\zeta})$ by $\frac{t}{t-pd} \text{trace}(\hat{\Sigma}_{\zeta})$, 16 can be written as

$$\mathbb{E}\|Y_{t+1} - \hat{Y}_{t+1}\|^2 \approx \frac{t + pd}{t - pd} \text{trace}(\hat{\Sigma}_{\zeta}) + \sum_{k>d} \lambda_k$$

Thus, the order p and the number of components d are simultaneously selected by minimizing the functional final perdition error criterion as

$$\text{FFPE}(p, d) = \frac{t + pd}{t - pd} \text{trace}(\widehat{\Sigma}_\zeta) + \sum_{k>d} \lambda_k. \quad (17)$$

The use of FFPE makes the forecasting procedure completely data-driven and does not require any subjective specification of parameters (see [39] for more technical details).

A flowchart of the proposed modeling framework using a separate or joint estimation approach is given in Figure 1. It explains that model estimation is a two-step procedure in the separate modeling approach, while all the components are modeled and forecasted in a single step in the joint approach.

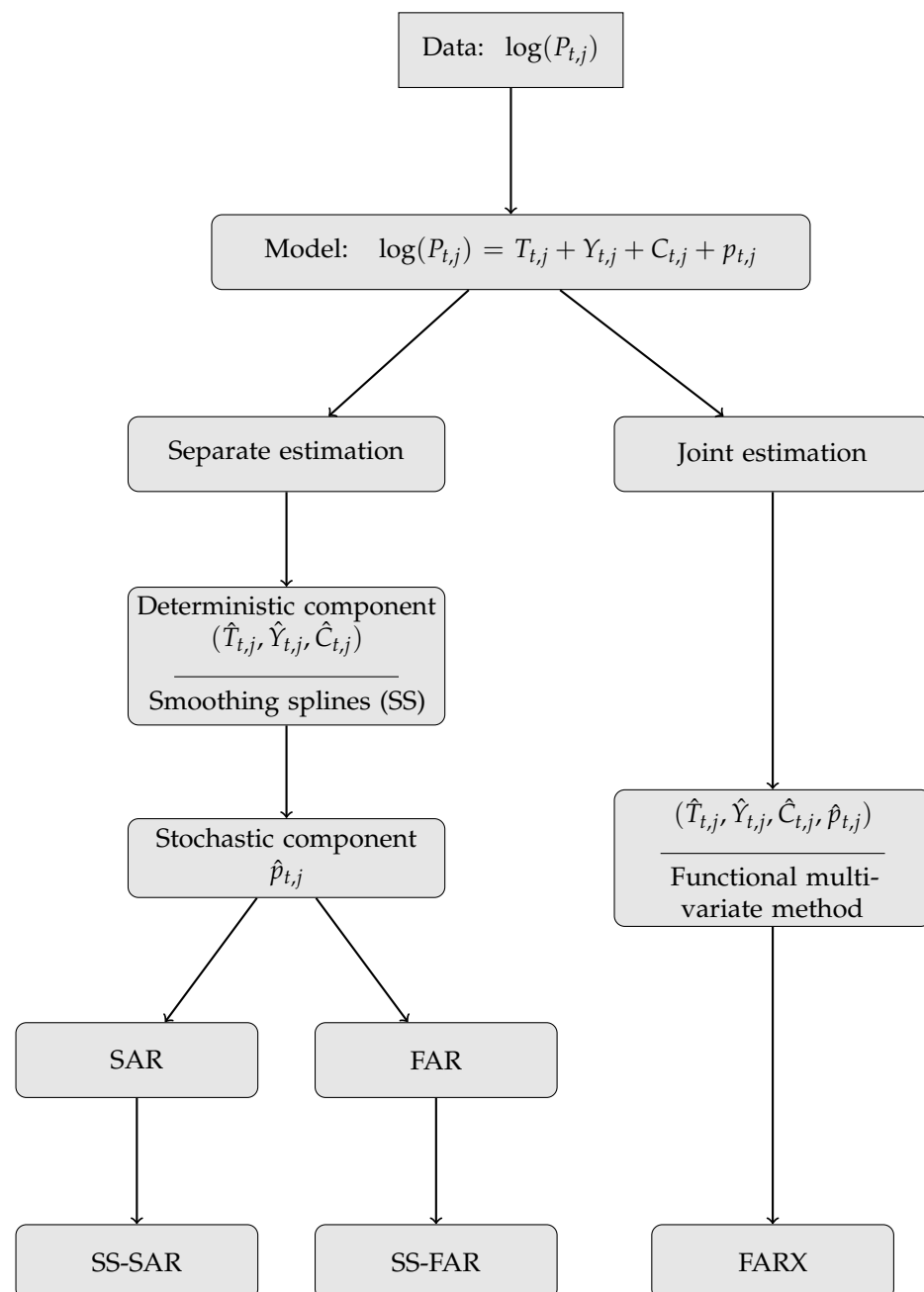


Figure 1. Flowchart of the general modeling framework.

4. Modeling and Forecasting IPEX Price for Northern Zone

4.1. Data

For an empirical investigation of the proposed methods, we consider the time series of the prices for the northern zone of the Italian electricity market (IPEX). The IPEX market is divided into zones, which are portions of the power grid where, for system security purposes, there are physical limits to transfers of electricity to/from other zones. They can be both geographical zones and virtual zones. In the period covered by the series, there were six geographical zones (see Figure 2) and the most important was the northern one (From the 1 January 2021, there are seven zones but the northern one is still the most important). The northern zone covers a wide range of geographical locations in Italy, so that it is difficult to exactly define longitude and latitude. However, roughly, longitude ranges from $7^{\circ}00'$ to $13^{\circ}40'$ east, while latitude from $44^{\circ}25'$ to $47^{\circ}00'$ north.



Figure 2. The six geographical zones of the IPEX market and the virtual zone of Rossano.

The data cover a period of five years ranging from 1 January 2015 to 31 December 2019. The data are plotted in Figure 3, where the purple line divides the in-sample period from the out-of-sample period. More precisely, data from 1 January 2015 to 31 December 2018 are used for model identification and estimation, while the whole year of 2019 is used for one-day-ahead out-of-sample forecasting.

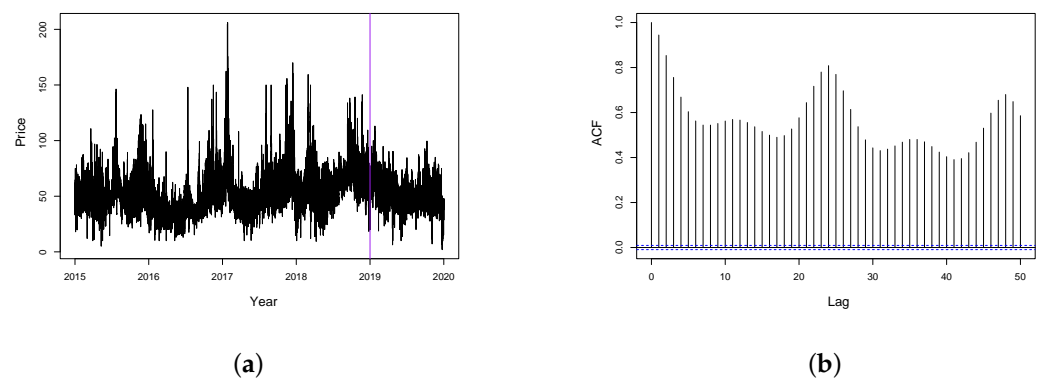


Figure 3. Electricity prices series for the northern Italian electricity market (a) and its autocorrelation function (b). The purple line distinguishes between model estimation and out-of-sample forecasting periods.

Some basic descriptive statistics for the data are listed in Table 2. The mean price is 52.34 EUR/MWh. Notably, the distribution appears to be slightly positively skewed, as suggested by the mean being higher than the median (50.16). Moreover, the standard deviation of 16.36 points out a non-negligible level of variability around the mean. Additionally, the first quartile at 41.36 EUR/MWh and the third quartile at 61.00 EUR/MWh help us understand where half of the values cluster within the dataset.

Table 2. Descriptive statistics for electricity prices data.

Min.	Q ₁	Median	Mean	Q ₃	SD	Max.
1.05	41.36	50.16	52.34	61.00	16.36	206.12

Figure 4 shows the daily functional trajectories, $Z_t(\tau)$ ($t = 1, 2, \dots, 1826$), of our time series. Here, each functional datum (curve) is evaluated at 24 points corresponding to hours of a day. Note that each day represents a single functional datum, facilitating us to evaluate them on a finer grid when required. This will lead us to obtain forecasts for ultra-short periods when needed. From the figure, it is quite clear that the daily price profiles show a considerable variation across time.

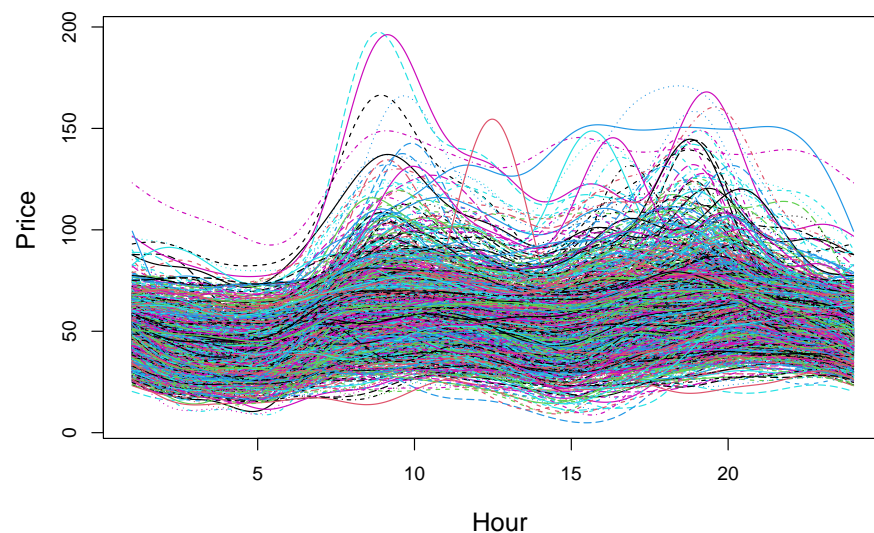


Figure 4. Functional daily trajectories $Z_t(\tau)$ for the original electricity prices.

4.2. Models Identification and Estimation

Since this work considers the model defined in (1), this section describes the model identification and estimation procedure in the cases of separate and joint estimation of the components described in Section 2.

Within the separate approach, the first step involved estimating the deterministic components. More specifically, the long-term and the periodic components were thought as deterministic functions of time, defined using cubic smoothing splines (SS). For calendar effects, instead, dummy variables were used. All these deterministic components were estimated by ordinary least squares methods, through the back-fitting algorithm. The weekly component $W_{t,j}$ was found to be non-significant and, therefore, was not included in the final model. This first step was performed separately for each univariate daily time series of the price of a specific load period. Once the deterministic components were estimated, the residual stochastic component, $p_{t,j}$ (see Figure 5 as an example), was modeled and predicted in two ways: using SARIMA models and FAR models. Figure 5 gives an example of the residual stochastic time series for the load period 10.

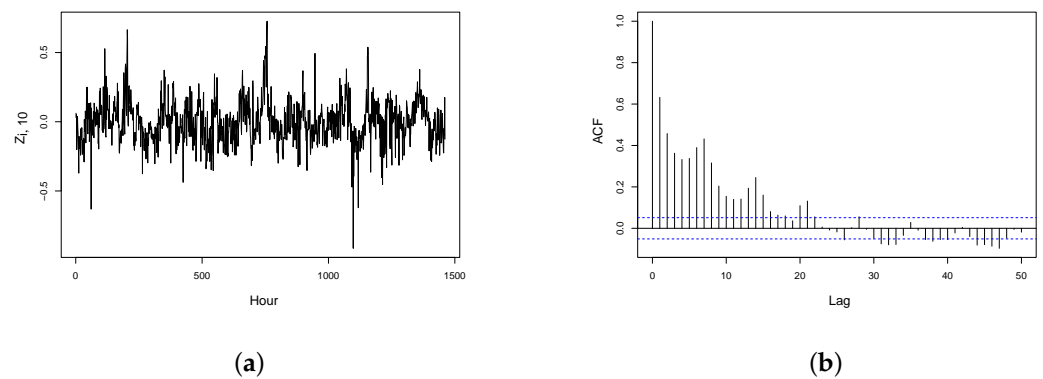


Figure 5. Stochastic component $p_{t,10}$ (a) and its ACF for load hour 10 (b).

The final prediction is then obtained, according to the formula (5), by summing all the specific components. To fit the FAR model, the series $p_{t,j}$ ($j = 1, \dots, 24$) are first converted to functional data using (4). As concerns SS-SARIMA, not all the series $p_{t,j}$ had the same autocorrelation structure. For most of them, the appropriate specification was a $SARIMA(3,0,0)(1,0,0)_7$ or, more shortly, $SAR(3,1)_7$ model; thus, we used it for all load periods. Note that the weekly component, which was not significant in the original data, is instead present in the residual component. Since both smoothing splines and the SARIMA model are used in this case, we refer to it as the SS-SARIMA model.

When the FAR model is applied, the series $p_{t,j}$ are first converted to functional objects using (4). The algorithm described in Section 3.3 was used to obtain the optimal values of the autoregressive order p and of the number of components d leading to white noise errors. We refer to this model as SS-FAR in order to stress the use of smoothing splines in the first step and of the FAR model in the second step.

In our case, the optimal values resulted to be $p = 5$ and $d = 10$. Thus, a FAR(5) model, based on 10 PCs, is used for out-of-sample forecasting.

In the case of joint estimation, we refer to the FARX model (14). The first step is to convert the original (log-)prices $\log(P_{t,j})$ into a functional object using (4). Again, the algorithm defined in Section 3.3 allows us to obtain p and d . For our data, the selected values were $p = 3$ and $d = 8$. We then used the deterministic components in their scalar form as exogenous variables. We could have also considered their functional specification but, being deterministic functions of time, forecasting results remain the same in both cases. This setting implies to fix $r = 4$ and bypasses the need of fixing the lag m or, equivalently, to fix $m = 0$. We denote this model as SS-FARX.

The ACFs and PACFs of the final residuals of the SS – $SAR(3,1)_7$, SS – FAR(5) and FARX(3,0,4) are shown in Figure 6. All models produce basically uncorrelated residuals but the FARX(3,0,4) model is clearly the best.

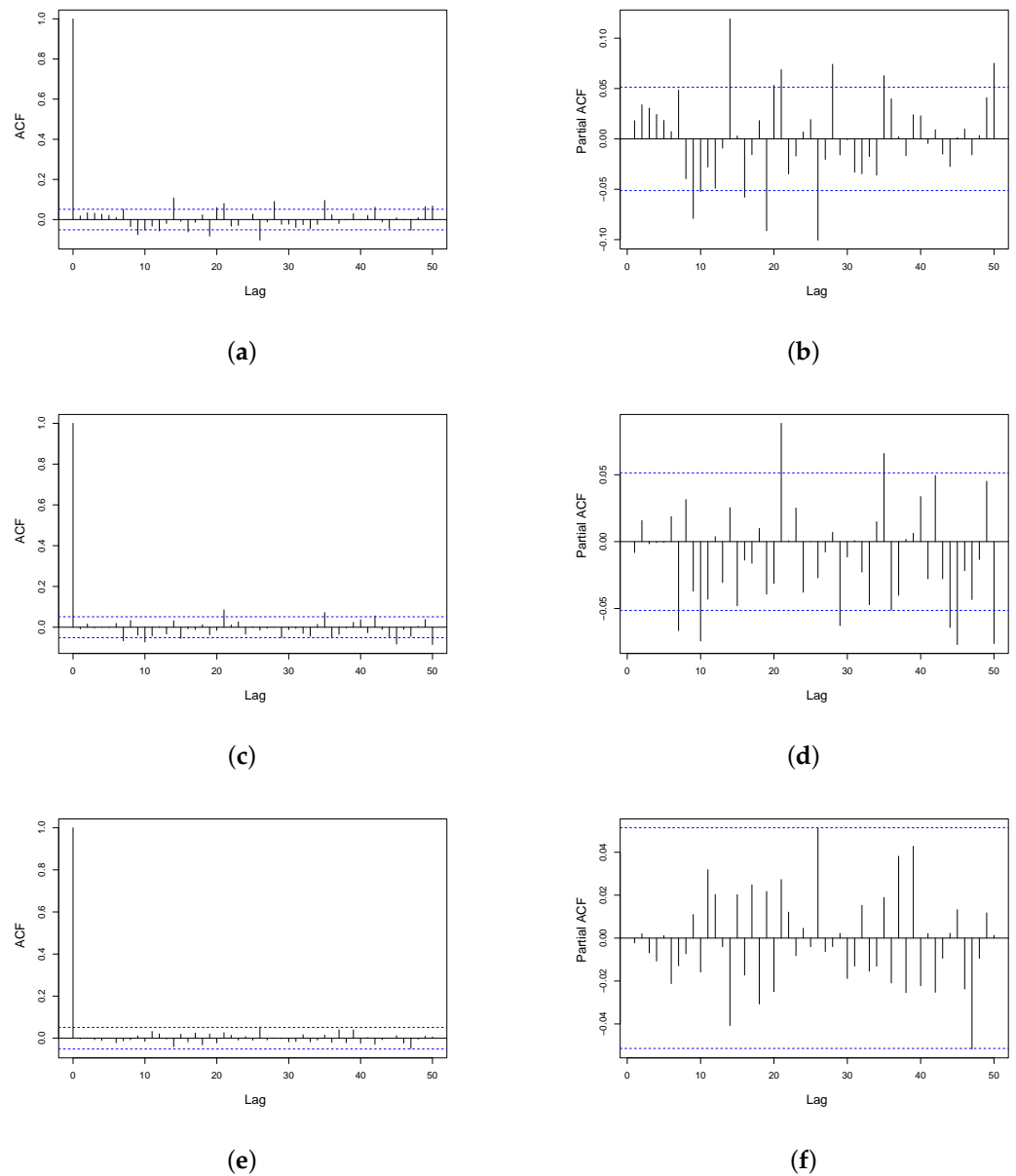


Figure 6. ACF and PACF for the final errors using models (a,b) SS-SAR(3,1)₇ (c,d) SS-FAR(5), and (e,f) FARX(3,0,4).

4.3. Out-of-Sample Forecasting

This section illustrates the forecasting performance of the models previously identified to make one-day-ahead price predictions. The comparison will be based both on descriptive indicators as well as using the Diebold and Mariano (1995) test, in order to assess the significance of the results.

More specifically, starting from 31 December 2018, we make $k = 365$ one-day-ahead predictions considering expanding windows. The models' specifications are those identified in the in-sample period and are kept fixed while the models' parameters are re-estimated day-by-day. All the variables were significant except the weekly component, W_t , which does not enter the models. In the separate modeling approach, the prediction is given by

$$\hat{P}_{t+1,j} = \exp\left(\hat{f}_1(T_{t+1}) + \hat{f}_2(Y_{t+1}) + \delta(C_{t+1}) + \hat{p}_{t+1,j}\right). \quad (18)$$

Predictions of the trend and of the yearly and weekly components, as well as of the bank holidays effect, are straightforward as soon as functions f_i and the parameter δ have been

estimated. The predictions $\hat{p}_{t+1}(j)$ were obtained using the SARIMA and FAR models. In the joint approach, predictions are directly made for the series of the price. In addition, we consider a fourth predictor obtained by combining the SS-FAR and the FARX models by means of a simple average of their forecasts [40,41]. For comparison purposes, two naïve models are also computed. The first model is called Naïve 1, which assumes that the next-day prices are equal to the current day, i.e., $\hat{P}_{t+1,j} = P_{t,j}$. The second model, Naïve 2, computes the next-day-ahead forecasts by assuming that tomorrow's electricity prices are the same as that of the previous week same day, i.e., $\hat{P}_{t+1,j} = P_{t-7,j}$, allowing for the incorporation of possible weekly periodicity in the forecasts [42].

To measure the forecasting error, we consider the mean absolute error (MAE), $(1/k) \sum (|P_{t,j} - \hat{P}_{t,j}|)$, the mean absolute percentage error (MAPE), $(1/k) \sum (|(P_{t,j} - \hat{P}_{t,j})/P_{t,j}|)$ and the root mean square error (RMSE) $[(1/k) \sum (P_{t,j} - \hat{P}_{t,j})^2]^{1/2}$, with $k = 365$ number of one-day-ahead predictions.

The forecasting results are summarized in Table 3, listing the predictive performance of the four models and two naïve benchmarks over the whole out-of-sample period, i.e., the year 2019. For all error measures, the best results are obtained by joint estimation through the FARX model. The second best result is that of the combination, which outperforms both the SS-SAR model and the SS-FAR model. From Table 3, it is also clear that models based on the functional approach perform better than the univariate SS-SAR model. More in detail, the MAE, MAPE, and RMSE values for the FARX(3,0,4) model are 4.25, 9.28, and 5.38. The percentage error reduction is about 20% with respect to SS-SAR(3,1) and about 10% with respect to SS-FAR(5). The indicators for FARX(3,0,4) and the combined predictor are quite similar. As the former model always gives better results, we attribute the good performance of the combined predictor to the contribution of the FARX model. Finally, the two benchmarks perform the worst compared to the four predictors, indicating the good performance of our models.

Table 3. One-day-ahead error measures for electricity price forecasting errors using the SS-SAR(3,1)₇ model, the SS-FAR(5) model, the FARX(3) model, the combined predictor and two naïve models.

Model	MAE	MAPE	RMSE
SS-SAR(3,1) ₇	5.12	11.51	6.99
SS-FAR(5)	4.57	10.17	6.23
FARX(3,0,4)	4.25	9.28	5.38
Combination	4.27	9.49	5.43
Naïve 1	8.39	18.75	11.41
Naïve 2	6.89	16.91	9.48

To assess the significance of the results listed in Table 3, the Diebold and Mariano (1995) test is applied to each couple of predictors. It has been applied to the squared errors to avoid the issues pointed out by [43]. The p -values of the tests are listed in Table 4. They refer to a hypothesis system whose null hypothesis assumes no difference in the accuracy of the forecasters in the row/column versus the alternative hypothesis that the forecaster in the row is more accurate than the forecaster in the column. The obtained p -values suggest that functional models are significantly more accurate than the univariate model. Within the functional approach, the FARX(3,0,4) produces statistically more accurate forecasts than the FAR(5) model but it is statistically equivalent to the combined predictor. However, as both the combination and FARX are significantly better than SS-FAR, as before, again we conclude that the contribution of the FARX model is crucial.

Table 4. p -values for the Diebold and Mariano test. The null hypothesis assumes equal prediction accuracy for the model in row and column, while the alternative hypothesis assumes the model in the row is more accurate than the model in the column.

Models	SS-SAR(3,1) ₇	SS-FAR(5)	FARX(3,0,4)	Combination	Naïve 1	Naïve 2
SS-SAR(3,1) ₇	-	>0.99	>0.99	>0.99	<0.01	<0.01
SS-FAR(5)	<0.01	-	>0.99	>0.99	<0.01	<0.01
SS-FARX(3)	<0.01	<0.01	-	0.14	<0.01	<0.01
Combination	<0.01	<0.01	0.86	-	<0.01	<0.01
Naïve 1	>0.99	>0.99	>0.99	>0.99	-	>0.99
Naïve 2	>0.99	>0.99	>0.99	>0.99	<0.01	-

Finally, the day-specific forecasting error indicators for the considered models are listed in Table 5. Looking at the table, we can see that Monday and Sunday typically have larger errors compared to other days of the week. On the contrary, Wednesday, Thursday, and Friday show lower forecasting errors, suggesting that prices are less erratic on these days. The FARX(3) model yields the lowest MAPE value of 7.85 on Thursday and the highest MAPE score of 12.32 on Saturday. Again, the FARX(3) model leads to uniformly better results over the days of the week. Analogous results for each month and each load period are listed in Tables A1 and A2 in the Appendix A. The results suggest that forecasting error depends on the load period, with peaks and lows at different times of the day. For example, the forecasting errors are particularly high from hour 3 to hour 6 in the morning and from 14 to 15 in the afternoon. On the other hand, errors are relatively lower from hour 20 to 1 a.m. Once again, the forecasting performance of the FARX(3) model produces, almost always, lower forecasting errors than the competitor models. In terms of monthly indicator the highest forecasting errors correspond to the months of June and December, while lower errors occur in January and February.

Table 5. Out-of-sample day-specific MAPE, MAE, RMSE for electricity price for SS-SAR(3,1)₇ model, SS-FAR(5) model, FARX(3,0,4) model, combination model, and two naïve benchmarks.

Model		Day of the Week						
		Mon	Tues	Wednes	Thurs	Fri	Satur	Sun
SS-SAR(3,1) ₇	MAE	6.09	5.37	5.14	4.57	4.47	4.89	5.21
SS-FAR(5)		5.07	4.82	4.77	4.32	4.40	4.11	4.54
FARX(3,0,4)		4.72	4.38	4.20	4.10	4.26	3.92	4.13
Combination		4.70	4.42	4.31	4.02	4.16	3.95	4.26
Naïve 1		6.52	7.05	9.44	8.36	5.88	10.59	10.94
Naïve 2		7.02	6.45	6.61	8.32	6.66	5.89	7.27
SS-SAR(3,1) ₇	MAPE	15.87	10.77	10.20	8.32	8.50	11.92	15.76
SS-FAR(5)		13.44	10.37	9.04	8.02	8.16	9.82	13.28
FARX(3,0,4)		12.32	9.67	8.15	7.85	8.07	8.96	10.84
Combination		12.57	9.75	8.34	7.64	7.85	9.27	11.91
Naïve 1		12.61	15.78	24.65	17.79	11.05	27.62	21.72
Naïve 2		13.32	14.19	23.14	23.17	12.38	16.45	15.45
SS-SAR(3,1) ₇	RMSE	8.13	7.66	7.29	6.34	6.00	6.31	6.81
SS-FAR(5)		6.72	7.07	6.67	5.79	5.77	5.35	6.04
FARX(3,0,4)		5.87	5.51	5.42	5.23	5.32	5.05	5.15
Combination		5.86	5.69	5.57	5.12	5.21	5.05	5.40
Naïve 1		7.97	8.34	11.13	9.88	7.32	12.59	13.10
Naïve 2		8.32	7.45	7.85	9.88	8.01	7.14	8.71

4.4. Computational Complexity

Finally, we compare the computational cost for each model used in our study. For the analyses, the programming environment R (R), a statistical computing language, is used to implement the models [44]. In the comparison, all the computations have been performed using an Intel(R)-Core(TM) i7-4770 CPU running at 3.40 GHz.

Table 6 provides the average time required for a one-day-ahead forecast for the different models. Using as a baseline the SS-SAR(3,1)₇ model, the average time required for a one-day-ahead forecast is 0.21 s, whereas the SS-FAR(5) and SS-FARX(3,0,4) models

take 0.72 and 0.77 s, respectively, for the same task. This means that SS-FAR(5) and SS-FARX(3,0,4) require 3.43 and 3.67 times more time needed compared to SS-SAR(3,1)₇. The combination model time is comparatively higher as both the models, SS-FAR(5) and SS-FARX(3,0,4), have to be computed. It is important to note that, except for the combination model, the models required less than a second to produce a one-day-ahead forecast, which suggests the models are quite computationally efficient.

To model and forecast the deterministic components when using a separate modeling approach, the *GAM* library in **R** was used [45]. The *forecast* library in **R** was used for the SAR model [46]. To estimate and forecast FAR(*p*) and FARX(*p*) models, the authors wrote their own code, which also used the **R** library *fda* [47]. The documentation provided by the packages provides in-depth details on the particular algorithms utilized in the estimation.

Table 6. Average time in seconds for a one-day-ahead forecast.

Average Time	SS-SAR(3,1) ₇	SS-FAR(5)	FARX(3,0,4)	Combination
Time (s)	0.21	0.72	0.77	1.52
Relative time	1	3.43	3.67	7.24

5. Conclusions

In this work, we faced the issue of modeling and forecasting electricity prices within the functional approach. As this is often conducted by estimating and predicting the different components of the price dynamics, we wondered if a joint modeling of the components could improve prediction with respect to a separate modeling process. The basic idea is that a joint estimation could consider those inter-relations among components that a separate modeling usually ignores. To investigate this issue, we compared the predictive performance of four different predictors: the first two are based on separate modeling, the third is based on joint modeling, and the fourth one is a combination of the two approaches.

In particular, the first two models use smoothing splines to estimate the deterministic components and SARIMA (SS-SAR) and FAR (SS-FAR) models to describe the dynamics of the stochastic component. The third model, the FARX model, follows a one-step procedure to jointly estimate all the components by suitably including exogenous variables. For empirical analysis, electricity price data from the northern zone of the Italian electricity market, from January 2015 to December 2019, are used. The first four years are used for model estimation, and the entire year 2019 is used for one-day-ahead out-of-sample forecasts. Forecasting performances are evaluated in terms of MAE, MAPE, and RMSE and statistically assessed by means of the Diebold and Mariano test.

The results suggest that the functional modeling approach is efficient in predicting electricity prices as it produces lower forecasting errors than the non-functional model used in the study, i.e., the SS-SAR model. Within the functional models, the FARX model, which jointly estimates all the components, significantly outperforms its competitors except the combined predictor. The last one, however, seems mainly affected by the good performance of the FARX model and gives numerical results worse than those of the FARX model.

Finally, this study's findings suggest that the forecasting errors are generally higher on (a) Sunday and Monday, (b) from hours 3 to 6 in the morning and 14 to 15 in the afternoon, and (c) June and December. On the other hand, prices are relatively lower on (a) Wednesday, Thursday, and Friday, (b) from hour 20 to 1 a.m., and (c) January and February.

Author Contributions: Conceptualization, F.L. and I.S.; methodology, F.L. and I.S.; software, I.S.; validation, F.L.; formal analysis, F.L. and I.S.; investigation, F.L. and I.S.; writing—original draft preparation, F.L. and I.S.; writing—review and editing, F.L. and I.S.; visualization, I.S.; supervision, F.L. All authors have read and agreed to the published version of the manuscript.

Funding: No specific funding was obtained for this research work.

Data Availability Statement: Data can be requested from the corresponding author(s).

Conflicts of Interest: There is no actual or potential conflict of interest concerning this article.

Appendix A

Table A1. Day-ahead price forecasting error indicators by month using the SS-SAR(3,1)₇, SS-FAR(5) and FARX(3,0,4) models.

Month		SS-SAR	SS-FAR	FARX	Month		SS-SAR	SS-FAR	FARX
Jan	MAE	5.63	5.78	4.77	Jul	MAE	5.44	4.31	4.33
	MAPE	8.76	8.99	7.37		MAPE	10.85	8.59	8.65
	RMSE	8.14	8.02	5.90		RMSE	6.96	5.51	5.51
Feb	MAE	4.76	3.97	3.91	Aug	MAE	5.05	3.96	3.96
	MAPE	9.20	7.67	7.07		MAPE	10.43	8.41	8.82
	RMSE	6.19	5.24	4.77		RMSE	7.33	5.49	5.19
Mar	MAE	4.70	4.33	4.14	Sep	MAE	4.70	4.33	4.14
	MAPE	9.21	8.38	8.02		MAPE	9.21	8.38	8.02
	RMSE	6.15	5.66	5.31		RMSE	6.15	5.66	5.31
Apr	MAE	5.78	5.86	4.53	Oct	MAE	5.46	4.88	4.26
	MAPE	12.74	12.59	9.50		MAPE	10.97	9.34	8.30
	RMSE	8.66	8.53	5.65		RMSE	7.15	6.58	5.50
May	MAE	4.31	3.99	4.05	Nov	MAE	4.69	4.42	4.19
	MAPE	9.00	8.18	8.41		MAPE	11.40	10.47	9.35
	RMSE	5.63	5.30	5.24		RMSE	6.26	5.87	5.30
June	MAE	5.34	4.70	4.52	Dec	MAE	4.73	4.45	4.26
	MAPE	14.29	12.24	11.11		MAPE	22.36	20.79	18.63
	RMSE	7.05	6.02	5.54		RMSE	6.33	5.76	5.29

Table A2. Day-ahead price forecasting error indicators by load period using the SS-SAR(3,1)₇, SS-FAR(5) and FARX(3,0,4) models.

Hour		SS-SAR	SS-FAR	FARX	Hour		SS-SAR	SS-FAR	FARX
1	MAE	4.21	3.53	3.28	13	MAE	4.84	4.67	4.47
	MAPE	10.35	8.86	7.59		MAPE	10.42	9.78	9.53
	RMSE	5.62	4.78	4.26		RMSE	6.48	6.02	5.64
2	MAE	4.28	3.41	3.26	14	MAE	5.49	4.96	4.58
	MAPE	11.86	9.95	9.16		MAPE	13.31	11.74	10.85
	RMSE	5.72	4.72	4.23		RMSE	7.62	6.64	5.80
3	MAE	4.38	3.57	3.43	15	MAE	6.48	5.74	4.61
	MAPE	14.71	12.32	11.10		MAPE	15.73	13.59	10.30
	RMSE	5.96	5.02	4.49		RMSE	8.90	7.90	5.72
4	MAE	4.49	3.84	3.64	16	MAE	6.32	5.84	4.89
	MAPE	17.53	15.33	13.98		MAPE	13.66	12.26	9.98
	RMSE	6.13	5.31	4.69		RMSE	8.55	7.88	6.07
5	MAE	4.43	3.85	3.64	17	MAE	6.09	5.55	5.14
	MAPE	17.67	15.83	14.59		MAPE	11.52	10.37	9.69
	RMSE	5.99	5.31	4.72		RMSE	8.24	7.45	6.47
6	MAE	4.17	3.68	3.34	18	MAE	5.69	5.16	4.85
	MAPE	13.86	12.87	10.33		MAPE	10.20	9.18	8.73
	RMSE	5.79	5.24	4.21		RMSE	7.58	6.77	6.03
7	MAE	5.14	4.17	4.00	19	MAE	5.41	5.09	4.90
	MAPE	12.37	9.84	8.73		MAPE	9.25	8.53	8.45
	RMSE	6.92	5.84	5.03		RMSE	7.14	6.47	6.02
8	MAE	5.68	4.69	4.34	20	MAE	5.00	4.81	4.62
	MAPE	11.59	9.27	8.85		MAPE	8.24	7.85	7.66
	RMSE	7.46	6.24	5.39		RMSE	6.59	6.28	5.67
9	MAE	6.99	5.79	4.85	21	MAE	4.64	4.68	4.58
	MAPE	13.23	10.65	9.08		MAPE	7.89	7.92	7.79
	RMSE	9.24	7.93	5.95		RMSE	6.04	5.94	5.62
10	MAE	6.59	5.46	5.17	22	MAE	4.21	4.40	4.12
	MAPE	12.41	10.05	9.44		MAPE	7.53	7.85	7.42
	RMSE	8.61	7.27	6.28		RMSE	5.63	5.68	5.09
11	MAE	5.86	5.07	4.85	23	MAE	3.44	3.37	3.33
	MAPE	11.04	9.36	9.31		MAPE	6.86	6.70	6.70
	RMSE	7.75	6.71	5.89		RMSE	4.73	4.64	4.45
12	MAE	5.89	5.28	4.76	24	MAE	3.12	3.38	3.45
	MAPE	11.56	10.10	9.39		MAPE	7.01	7.65	7.83
	RMSE	7.88	6.97	5.82		RMSE	4.05	4.43	4.48

References

1. Lago, J.; Marcjasz, G.; De Schutter, B.; Weron, R. Forecasting day-ahead electricity prices: A review of state-of-the-art algorithms, best practices and an open-access benchmark. *Appl. Energy* **2021**, *293*, 116983. [[CrossRef](#)]
2. Lisi, F.; Nan, F. Component estimation for electricity prices: Procedures and comparisons. *Energy Econ.* **2014**, *44*, 143–159. [[CrossRef](#)]
3. Nowotarski, J.; Weron, R. Recent advances in electricity price forecasting: A review of probabilistic forecasting. *Renew. Sustain. Energy Rev.* **2018**, *81*, 1548–1568. [[CrossRef](#)]
4. Shah, I.; Iftikhar, H.; Ali, S.; Wang, D. Short-term electricity demand forecasting using components estimation technique. *Energies* **2019**, *12*, 2532. [[CrossRef](#)]
5. Liu, J.M.; Chen, R.; Liu, L.M.; Harris, J.L. A semi-parametric time series approach in modeling hourly electricity loads. *J. Forecast.* **2006**, *25*, 537–559. [[CrossRef](#)]
6. Zhang, J.L.; Zhang, Y.J.; Li, D.Z.; Tan, Z.F.; Ji, J.F. Forecasting day-ahead electricity prices using a new integrated model. *Int. J. Electr. Power Energy Syst.* **2019**, *105*, 541–548. [[CrossRef](#)]
7. Vilar, J.M.; Cao, R.; Aneiros, G. Forecasting next-day electricity demand and price using nonparametric functional methods. *Int. J. Electr. Power Energy Syst.* **2012**, *39*, 48–55. [[CrossRef](#)]
8. García-Martos, C.; Rodríguez, J.; Sánchez, M.J. Forecasting electricity prices and their volatilities using Unobserved Components. *Energy Econ.* **2011**, *33*, 1227–1239. [[CrossRef](#)]
9. Kostrzewski, M.; Kostrzewska, J. Probabilistic electricity price forecasting with Bayesian stochastic volatility models. *Energy Econ.* **2019**, *80*, 610–620. [[CrossRef](#)]
10. Kristiansen, T. Forecasting Nord Pool day-ahead prices with an autoregressive model. *Energy Policy* **2012**, *49*, 328–332. [[CrossRef](#)]
11. Koopman, S.J.; Ooms, M.; Carnero, M.A. Periodic seasonal Reg-ARFIMA–GARCH models for daily electricity spot prices. *J. Am. Stat. Assoc.* **2007**, *102*, 16–27. [[CrossRef](#)]
12. Girish, G.P. Spot electricity price forecasting in Indian electricity market using autoregressive-GARCH models. *Energy Strategy Rev.* **2016**, *11*, 52–57. [[CrossRef](#)]
13. Conejo, A.J.; Contreras, J.; Espínola, R.; Plazas, M.A. Forecasting electricity prices for a day-ahead pool-based electric energy market. *Int. J. Forecast.* **2005**, *21*, 435–462. [[CrossRef](#)]
14. Taylor, J.W. Short-term electricity demand forecasting using double seasonal exponential smoothing. *J. Oper. Res. Soc.* **2003**, *54*, 799–805. [[CrossRef](#)]
15. Heidarpanah, M.; Hooshyaripor, F.; Fazeli, M. Daily electricity price forecasting using artificial intelligence models in the Iranian electricity market. *Energy* **2023**, *263*, 126011. [[CrossRef](#)]
16. Gomez, W.; Wang, F.K.; Amogne, Z.E. Electricity Load and Price Forecasting Using a Hybrid Method Based Bidirectional Long Short-Term Memory with Attention Mechanism Model. *Int. J. Energy Res.* **2023**, *2023*, 3815063. [[CrossRef](#)]
17. Menéndez Medina, A.; Heredia Álvaro, J.A. Using Generative Pre-Trained Transformers (GPT) for Electricity Price Trend Forecasting in the Spanish Market. *Energies* **2024**, *17*, 2338. [[CrossRef](#)]
18. Dudek, G. Short-term load forecasting using random forests. In *Intelligent Systems' 2014*; Springer: Berlin/Heidelberg, Germany, 2015; pp. 821–828.
19. Aggarwal, S.; Saini, L.; Kumar, A. Day-ahead price forecasting in Ontario electricity market using variable-segmented support vector machine-based model. *Electr. Power Compon. Syst.* **2009**, *37*, 495–516. [[CrossRef](#)]
20. Amjady, N. Day-ahead price forecasting of electricity markets by a new fuzzy neural network. *IEEE Trans. Power Syst.* **2006**, *21*, 887–896. [[CrossRef](#)]
21. Tan, M.; Hu, C.; Chen, J.; Wang, L.; Li, Z. Multi-node load forecasting based on multi-task learning with modal feature extraction. *Eng. Appl. Artif. Intell.* **2022**, *112*, 104856. [[CrossRef](#)]
22. Shang, Y.; Li, S. FedPT-V2G: Security enhanced federated transformer learning for real-time V2G dispatch with non-IID data. *Appl. Energy* **2024**, *358*, 122626. [[CrossRef](#)]
23. Bai, M.; Yao, P.; Dong, H.; Fang, Z.; Jin, W.; Yang, X.; Liu, J.; Yu, D. Spatial-temporal characteristics analysis of solar irradiance forecast errors in Europe and North America. *Energy* **2024**, *297*, 131187. [[CrossRef](#)]
24. Chaouch, M. Clustering-based improvement of nonparametric functional time series forecasting: Application to intra-day household-level load curves. *IEEE Trans. Smart Grid* **2013**, *5*, 411–419. [[CrossRef](#)]
25. Paparoditis, E.; Sapatinas, T. Short-term load forecasting: The similar shape functional time-series predictor. *IEEE Trans. Power Syst.* **2013**, *28*, 3818–3825. [[CrossRef](#)]
26. Marcjasz, G.; Narajewski, M.; Weron, R.; Ziel, F. Distributional neural networks for electricity price forecasting. *Energy Econ.* **2023**, *125*, 106843. [[CrossRef](#)]
27. Cruz, A.; Muñoz, A.; Zamora, J.L.; Espínola, R. The effect of wind generation and weekday on Spanish electricity spot price forecasting. *Electr. Power Syst. Res.* **2011**, *81*, 1924–1935. [[CrossRef](#)]
28. Shah, I.; Bibi, H.; Ali, S.; Wang, L.; Yue, Z. Forecasting one-day-ahead electricity prices for Italian electricity market using parametric and nonparametric approaches. *IEEE Access* **2020**, *8*, 123104–123113. [[CrossRef](#)]
29. Conejo, A.J.; Plazas, M.A.; Espinola, R.; Molina, A.B. Day-ahead electricity price forecasting using the wavelet transform and ARIMA models. *IEEE Trans. Power Syst.* **2005**, *20*, 1035–1042. [[CrossRef](#)]

30. Bibi, N.; Shah, I.; Alsubie, A.; Ali, S.; Lone, S.A. Electricity spot prices forecasting based on ensemble learning. *IEEE Access* **2021**, *9*, 150984–150992. [[CrossRef](#)]
31. Lisi, F.; Pelagatti, M.M. Component estimation for electricity market data: Deterministic or stochastic? *Energy Econ.* **2018**, *74*, 13–37. [[CrossRef](#)]
32. Stark, H.; Woods, J.W. *Probability, Random Processes, and Estimation Theory for Engineers*; Prentice-Hall, Inc.: Hoboken, NJ, USA, 1986.
33. Ramsay, J.O.; Silverman, B.W. *Applied Functional Data Analysis: Methods and Case Studies*; Springer: Berlin/Heidelberg, Germany, 2002; Volume 77.
34. Shang, H.L. A survey of functional principal component analysis. *ASTA Adv. Stat. Anal.* **2014**, *98*, 121–142. [[CrossRef](#)]
35. Hörmann, S.; Kokoszka, P. Weakly dependent functional data. *Ann. Stat.* **2010**, *38*, 1845–1884. [[CrossRef](#)]
36. Bosq, D. *Linear Processes in Function Spaces: Theory and Applications*; Springer Science & Business Media: Berlin/Heidelberg, Germany, 2000; Volume 149.
37. Mourid, T. Processus autorégressifs banachiques d'ordre supérieur. *Comptes Rendus L'Academie Sci. Ser. 1 Math.* **1993**, *317*, 1167–1172.
38. Lutkepohl, H. *New Introduction to Multiple Time Series Analysis*; Springer: Berlin/Heidelberg, Germany, 2006.
39. Aue, A.; Norinho, D.D.; Hörmann, S. On the prediction of stationary functional time series. *J. Am. Stat. Assoc.* **2015**, *110*, 378–392. [[CrossRef](#)]
40. Stock, J.H.; Watson, M.W. Forecasting with many predictors. *Handb. Econ. Forecast.* **2006**, *1*, 515–554.
41. Bordignon, S.; Bunn, D.W.; Lisi, F.; Nan, F. Combining day-ahead forecasts for British electricity prices. *Energy Econ.* **2013**, *35*, 88–103. [[CrossRef](#)]
42. Mandal, P.; Senjyu, T.; Urasaki, N.; Funabashi, T.; Srivastava, A.K. A novel approach to forecast electricity price for PJM using neural network and similar days method. *IEEE Trans. Power Syst.* **2007**, *22*, 2058–2065. [[CrossRef](#)]
43. Franses, P.H. A note on the mean absolute scaled error. *Int. J. Forecast.* **2016**, *32*, 20–22. [[CrossRef](#)]
44. R Core Team. *R: A Language and Environment for Statistical Computing*; R Foundation for Statistical Computing: Vienna, Austria, 2013.
45. Hastie, T. *Gam: Generalized Additive Models*, R package version 1.22; Elsevier: Amsterdam, The Netherlands, 2022.
46. Hyndman, R.J.; Khandakar, Y. Automatic time series forecasting: The forecast package for R. *J. Stat. Softw.* **2008**, *27*, 1–22. [[CrossRef](#)]
47. Ramsay, J.O.; Graves, S.; Hooker, G. *Fda: Functional Data Analysis*, R package version 5.1.7; IEEE: New York, NY, USA, 2020.

Disclaimer/Publisher's Note: The statements, opinions and data contained in all publications are solely those of the individual author(s) and contributor(s) and not of MDPI and/or the editor(s). MDPI and/or the editor(s) disclaim responsibility for any injury to people or property resulting from any ideas, methods, instructions or products referred to in the content.